

Accuracy of Enhanced Distance Active Contour (EDAC) for Microcalcifications Segmentation

Siti Salmah Yasiran¹, Wan Eny Zarina Wan Abdul Rahman¹, Arsmah Ibrahim¹, Abdul Kadir
Jumaat¹, and Rozi Mahmud²

¹ Faculty of Computer and Mathematical Sciences
Universiti Teknologi MARA, 40450 Shah Alam, Selangor, Malaysia.

² Faculty of Medicine
Universiti Putra Malaysia, 43400 Serdang, Selangor, Malaysia.

Abstract. Boundaries of microcalcification segmented using the Distance Active Contour (DAC) method produces low accuracy. In this paper the Enhanced Distance Active Contour (EDAC) is proposed to overcome the problem. The accuracy is measured by using the Receiver Operating Characteristic (ROC) Curve. The values of True Positive, True Negative, False Positive, and False Negative based on the EDAC segmentation results are benched by radiologists. Results obtained show that the Area Under the Curve (AUC) of the ROC is numerically found to be 0.84 in value which verifies that EDAC produces high accuracy.

Keywords: Enhanced Distance Active Contour, Mammogram, Microcalcifications, Segmentation, Boundaries.

1. Introduction

Snake or Active Contour [1] which is computational in nature has been widely used in many applications of computer vision and image processing. It is a segmentation technique which is composed of computer generated curves that move within images to segment the image boundaries. Image segmentation has become increasingly significant and challenging tasks in the medical imaging such as mammogram, Magnetic Resonance Imaging (MRI) and Computed Tomography (CT) over the past two decades. The Distance Active Contour (DAC) is originally proposed by Xu & Prince [2]. However, the DAC results show low performance in terms of accuracy. Therefore our proposed method which is called the Enhanced Distance Active Contour (EDAC) is introduced in order to solve the issue. In this paper, the accuracy of DAC and EDAC in segmenting characteristic details on breast phantom images is compared.

The breast phantom refers to a test object used to simulate radiographic characteristics of compressed tissue. A phantom is designed to simulate x-ray attenuation of 4.2 cm compressed human breast which is composed of 50% adipose and 50% glandular tissue. In this paper, the breast phantom is needed in order to test the applicability of EDAC, in the detection of the characteristic details in the phantom. Once the application on DAC and EDAC is completed, both methods are implemented on mammograms to segment microcalcifications [3]. Finally, the performance of both methods are measured and compared. This is to verify that the efficiency of EDAC is better than DAC.

1.1.1. The Enhanced Distance Active Contour (EDAC)

Active Contour or snake [1] is an energy minimizing spline guided by external forces and influenced by image forces, which pull it towards features such as boundaries, edges and lines [4]. Active Contour has been

⁺ Corresponding author. Tel.: (+6014-3384203) fax: (+603-55435301)

E-mail address: (sitisalmah@tmsk.uitm.edu.my).

extensively used to extract the boundaries of an object such as in image segmentation [5,6,7] image tracking [8] and 3-D reconstruction [9]. Active Contour [1] is represented by parametric curve $v(s)=[x(s),y(s)]$, $s \in [0,1]$ with x and y as the coordinates of vertices. In simple word, the Active Contour refers to an elastic curve driven by energy generated from that image. The image is processed to generate a potential field which makes the model active. The Active Contour moves into alignment with the local energy minimum of an image features of an edge. The curve moves through the spatial domain of an image to minimize the energy function which can be represented mathematically as:

$$E_{AC} = \int_0^1 [E_{int} v(s) + E_{ext} v(s)] ds \quad (1)$$

The first term E_{int} of Equation (1) represents the internal energy which is responsible for the smoothness and deformation process of the contour and can be expressed as:

$$E_{AC} = \int_0^1 \frac{1}{2} [\alpha |v_s(s)|^2 + \beta |v_{ss}(s)|^2 + E_{ext} v(s)] ds \quad (2)$$

where $\alpha(s)$ and $\beta(s)$ are the elasticity and rigidity parameter respectively. The external energy function E_{ext} attracts the deformable contour to the boundary or edge of the image. By using calculus of variations, an Active Contour that minimizes the energy functional in Equation (2) must satisfy the Euler-Lagrange equation which can be expressed as:

$$\alpha v_{ss}(s) - \beta v_{ssss}(s) - \nabla E_{ext} = 0 \quad (3)$$

The Finite Difference Method (FDM) is selected due to its simplicity [10]. In this paper, the DAC is chosen since it is not well explored. No literature has been found so far whereby the method is implemented on mammogram. For instance, Xu & Prince [2] introduced the GVF Active Contour as well as the DAC and made some comparison. It is found that the GVF Active Contour performs much better. Then, another paper is done by the same researcher where GGVF Active [6] is proposed to improve the GVF Active Contour. As a different approach, Hou & Han [10] used the distance Potential force as the external force to create the Fast Force Analysis (FFA) Active Contour. Another creative idea carried by Sum & Cheung [11] which associated with potential force by replacing the original potential force with its norm. The DAC requires longer computational time to complete the segmentation process. Thus, some enhancement should be made to overcome this issue. The pseudo codes of the EDAC are illustrated in Figure 1:

```

get g = image_file;
set h = 200_by_200_pxl;
set f = edge_map ; f = 1- [g / 255];
    % replaced with canny edge detection;
set D = sqrt(f((x2-x1)^2) + f((y2-y1)^2)) > 0.5;
set [p_x p_y] = gradient(-D); j = [p_x p_y];
set the initialization;
while [ i <= xi ] {
    if [[ x < h ] && [ y < h ] ] {
        j = EDAC_deform ;
    }
}
display j ;

```

Fig.1. The pseudo codes of the EDAC

The first step is to read the image file. Then, the edge map is computed. The inverse edge map method is used in the original algorithm. However, this method requires a long time to complete the segmentation process. Hence, this part is modified in order to reduce the time to complete the segmentation process. The Canny edge map is chosen to replace the inverse method. This is because Canny edge detector is one of the most powerful edge detection methods to detect object boundaries [12]. The next step is to compute the external force based on the computed edge map. The Euclidean distance formula is used to compute the

distance. Next, the initialization is defined. Then the number of iterations is denoted by the parameter ξ which is also known as the stopping criteria for the iterations process. The iteration continues until it reaches this stopping criterion.

1.1.2. Materials and Methods

This paper is mainly divided into four major stages. The first stage is data collection. Original mammogram images are obtained from National Cancer Society Malaysia (NCSM). Since this study is attempted to show the applicability of new algorithm of EDAC in segmenting the microcalcifications, we will only focus on the Region of Interest (ROI). In this case, the radiologist will confirm the ROI first.

The second stage is the enhancement of DAC. It will be tested first on a breast phantom. If the modified algorithm satisfies the scoring criteria set by ACR [13], then it will be used in the next phase. Otherwise, some modifications on the algorithm will be made until the scoring criteria set by ACR are satisfied. According to ACR, if the total scoring is less than 10 then it means that the algorithm provides a poor image quality. Thus, the scoring must be greater than 10 in order to obtain a good image quality [13]. A paper on the breast phantom associated with the Active Contour or snake algorithm has been successfully conducted by Wan Eny Zarina et al. [14]. The finding shows that the implementation of the Active Contour on the partitions of image of breast phantom image is able to increase the sensitivity of detection of characteristic details of breast phantom. Thus, in this paper the experiments are conducted on the partition of the breast phantom image. The next stage is the implementation of the EDAC on the mammograms. The final stage is to measure the accuracy of the EDAC. Figure 2 illustrates the block diagram of our proposed method.

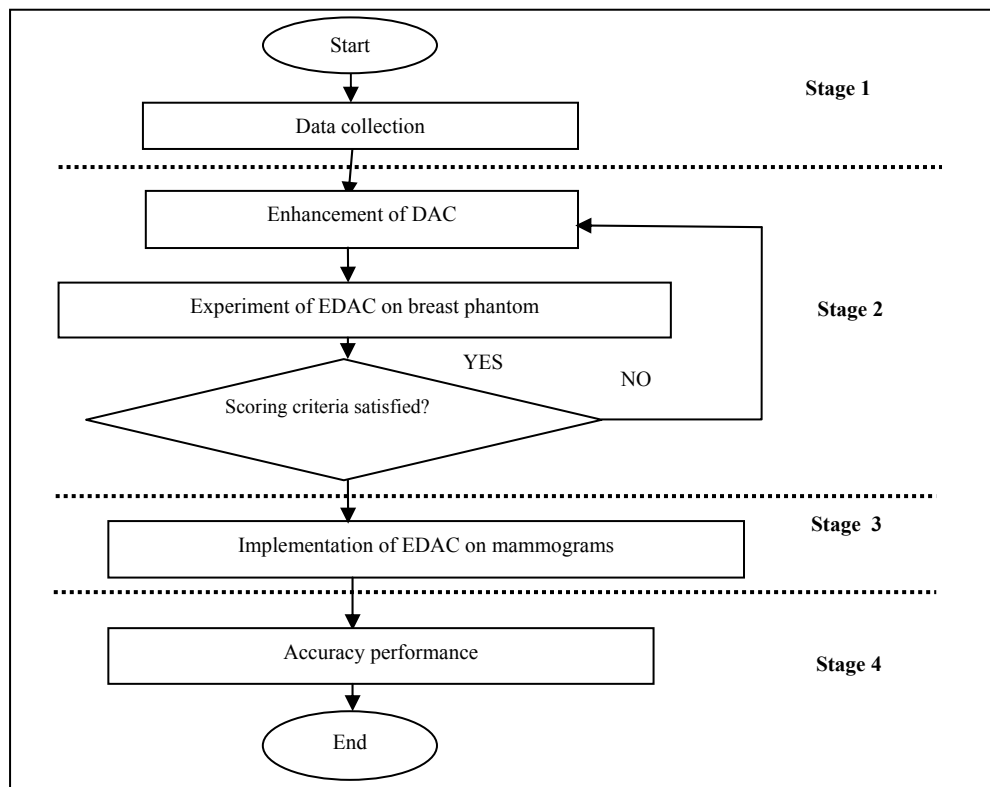


Fig.2. The block diagram of EDAC

1.1.3. Experimental Results

1.1.4. Breast Phantom

To test the capability of the EDAC it is implemented on the phantom to trace the hidden characteristic details. A scoring is performed on the merged phantom before and after implementing the EDAC by a radiologist. Tables 1 (a) and (b) illustrate the scoring results obtained by the radiologist.

Table 1 (a). Scoring phantom before EDAC

Characteristic Details	Top Left	Bottom Left	Top Right	Bottom Right
Fibrils	2	2	0	0
Specks	1	0	0	0
Mass	1	0	1	2
Subtotal	4	2	1	2
OVERALL TOTAL	4+2+1+2=9			

Table 1 (b). Scoring phantom after EDAC

Characteristic Details	Top Left	Bottom Left	Top Right	Bottom Right
Fibrils	2	2	0	0
Specks	2	1	0	0
Mass	1	2	2	2
Subtotal	5	5	2	2
OVERALL TOTAL	5+5+2+2=14			

From both Tables 1 (a) and (b), it is found that the total scoring for the phantom before implementing the EDAC is 9. This shows that the phantom did not meet the criteria of the good image quality. Meanwhile, the total scoring for the phantom after implementing the EDAC is 14. These results fully satisfied all the criteria for good image quality. Besides, the total number of characteristic details detected by using EDAC is 14 which exceed 10 in number. According to ACR this result represents a good image quality. These results confirm that the EDAC algorithm is highly suitable to segment microcalcifications directly on the mammograms.

1.1.5. Accuracy of EDAC

The accuracy is measured based on the value of AUC in the ROC curve. Then, the sensitivity and specificity of each reading from radiologists and EDAC is calculated. The ROC curves in Figure 3 below show the tradeoff between the sensitivity and specificity.

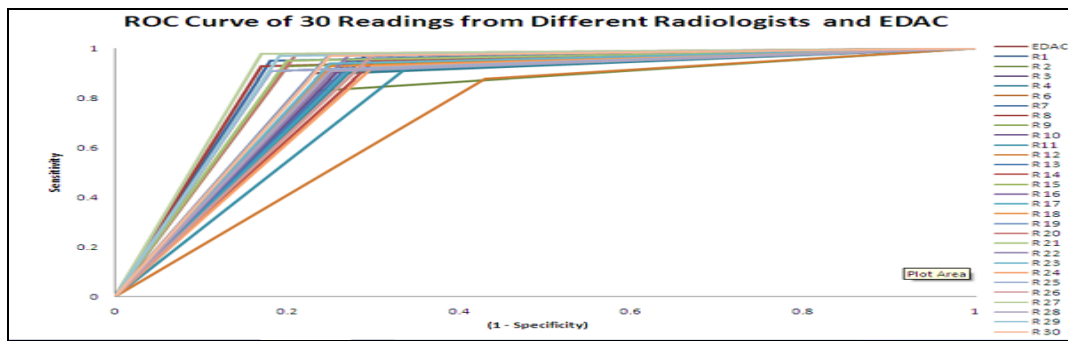


Fig. 3. ROC curves of 30 readings from different radiologists and EDAC

It can be observed that all the ROC curves obtained from EDAC and each radiologist lie well above the diagonal line connecting point (0,0) and (1,1). It can be concluded that EDAC is accurate. To verify this, the value of AUC is obtained from 30 different radiologists and the value is plotted as is in Figure 4.

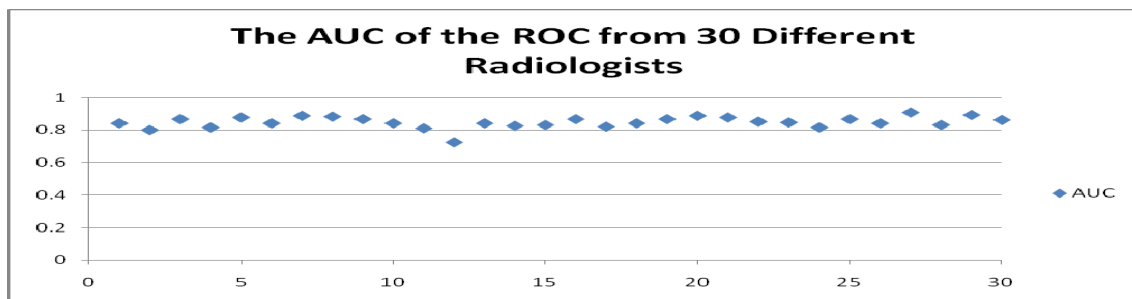


Fig. 4. The value of AUC of the ROC from 30 different radiologist

The AUC of EDAC is 0.84. Meanwhile, the AUC of the DAC is 0.78. As illustrated in Figure 4, the AUC of the ROC of each radiologist readings and EDAC are almost similar and approach to '1'. According to Hanely *et al.*, [15], these values verify the accuracy of EDAC is high compared to the DAC.

2. Acknowledgements

The author would like to acknowledge the Universiti Teknologi MARA for the support and contributions.

3. References

- [1] Kass, M., Witkin, A. & Terzopoulos, D. (1987). Snakes: Active Contour models. *International Journal Computer Vision* , vol. 1, 321-331.
- [2] Xu, C. & Prince, J.L. (March 1998 (a)). Snake, shape and gradient vector flow. *IEEE Trans. on Image Process.* , 359-369.
- [3] *Administrative Code*. (2005). Retrieved July 17, 2009, from facilities performing mammography Section 370.20 definitions: <http://www.ilga.gov/commission/jcar/admincode/032/032003700000200R.html>
- [4] Xie, X. (May 2002). *Interim Report: Active Colour Snakes*. University of Bristol.
- [5] Yezzi, A., Kichenassamy, S., Kumar, A., & Tannenbaum, A. (1997). A geometric snake model for segmentation medical imagery. *IEEE transaction on the medical imaging* , 16, 199-209.
- [6] Xu, C. & Prince, J.L. (1998 (b)). Generalized gradient vector flow external forces for Active Contours. *Elsevier: Signal processing* , 71, 131-139.
- [7] Brigger, P., Hong, J., Unser, M. (2000). B-Spline snakes: Aflexible tool for parametric contour detection. *IEEE Transaction Image Processing* , 9 (9),
- [8] Leymarie, F. & Levine, M.D. (1993). Tracking deformable objects in the plane using an Active Contour models. *IEEE Trans. Pattern. Anal. Mach. Intell.* , 15 (6), 617-634.
- [9] Cohen, L.D., & Cohen, I. (1993). Finite element methods for Active Contour models and balloons for 2-D and 3-D images. *IEEE Trans. Pattren Anal. Mach. Intell*, 15, 1131-1147.
- [10] Hou, Z., & Han, C. (200). Force field analysis snake: an improved parametric active contour model. *Elsevier: Pattern recognition letters* , 26, 513-526.
- [11] Sum, K.W. & Cheung, P.Y.S. (2007). Boundary vector field for parametric active contours. *Elsevier: Pattern recognition* , 40, 1635-1645.
- [12] Canny, J.F. (1986). A Computational Approach to Edge Detection. *IEEE Trans on PAMI* , 8 (6), 679-698.
- [13] American College of Radiology Mammography Accreditation. (2009, April 4) Retrieved June 25, 2009, from PDF File: http://www.acr.org/accreditation/mammography/mammo_faq/mammo_faq.aspx
- [14] Wan Eny Zarina, W.A. R., Arsmah, I., Zainab, A. B., Rozi, M.,Md. Saion, S., & Mazani, M. (2008). Post Processing of Breast Phantom MRI-156 Images Using Snake Algorithm. *IEEE : Fifth International Conference on Computer Graphics, Imaging and Visualization*.
- [15] Hanely J.A., Barbara, J., & McNeil M.D., (1982). The meaning and use of the area under the receiver operating characteristic (ROC) curve. *Radiology* , 143, 29-36.